



# Immunoengineering nerve repair

Nassir Mokarram<sup>a,1</sup>, Kyle Dymanus<sup>b</sup>, Akhil Srinivasan<sup>b,c</sup>, Johnathan G. Lyon<sup>a,b,c</sup>, John Tipton<sup>b</sup>, Jason Chu<sup>b,d</sup>, Arthur W. English<sup>e</sup>, and Ravi V. Bellamkonda<sup>a,1</sup>

<sup>a</sup>Department of Biomedical Engineering, Pratt School of Engineering, Duke University, Durham, NC 27708; <sup>b</sup>Wallace H. Coulter Department of Biomedical Engineering, Georgia Institute of Technology, Atlanta, GA 30332; <sup>c</sup>Wallace H. Coulter Department of Biomedical Engineering, Emory University, Atlanta, GA 30322; <sup>d</sup>Department of Neurosurgery, Emory University School of Medicine, Atlanta, GA 30307; and <sup>e</sup>Department of Cell Biology, Emory University, Atlanta, GA 30332

Edited by Robert Langer, MIT, Cambridge, MA, and approved May 11, 2017 (received for review April 12, 2017)

Injuries to the peripheral nervous system are major sources of disability and often result in painful neuropathies or the impairment of muscle movement and/or normal sensations. For gaps smaller than 10 mm in rodents, nearly normal functional recovery can be achieved; for longer gaps, however, there are challenges that have remained insurmountable. The current clinical gold standard used to bridge long, nonhealing nerve gaps, the autologous nerve graft (autograft), has several drawbacks. Despite best efforts, engineering an alternative “nerve bridge” for peripheral nerve repair remains elusive; hence, there is a compelling need to design new approaches that match or exceed the performance of autografts across critically sized nerve gaps. Here an immunomodulatory approach to stimulating nerve repair in a nerve-guidance scaffold was used to explore the regenerative effect of reparative monocyte recruitment. Early modulation of the immune environment at the injury site via fractalkine delivery resulted in a dramatic increase in regeneration as evident from histological and electrophysiological analyses. This study suggests that biasing the infiltrating inflammatory/immune cellular milieu after injury toward a proregenerative population creates a permissive environment for repair. This approach is a shift from the current modes of clinical and laboratory methods for nerve repair, which potentially opens an alternative paradigm to stimulate endogenous peripheral nerve repair.

immunomodulation | nerve repair | monocyte | macrophage | fractalkine

Peripheral nervous system (PNS) injuries lead to long-term disability and decreased function in ~2.8% of all trauma patients (1), and are often followed by neuropathic pain that significantly affects the quality of life for individuals suffering from these injuries. Many of the current surgical techniques for repairing these nerve injuries were developed during World Wars I and II in the first half of the 20th century. With the advent of microsurgical techniques, some progress has been achieved in the field of nerve repair (2), however bridging of long peripheral nerve gaps remains a continuing clinical challenge (3).

After nerve trauma, the standard clinical operating procedure is to oppose the two nerve ends and, when possible, suture them together. If the gap is large enough that tensionless apposition is not possible, an autologous nerve graft (autograft) (3, 4), typically the patient’s own sural nerve, or, more recently, a cadaver-derived graft (allograft) is used to bridge the nerve gap (5, 6). Autografts are biocompatible, nontoxic, and supportive of the structures that promote axonal adhesion/extension. Although they are currently the best clinical bridges available, they suffer from some major drawbacks such as the need for a secondary surgery, limitations in the availability of disposable nerve segments, and the possibility of neuroma formation (3). Allograft use affords improved presurgical sourcing and preparation but also entails a higher chance of immunogenicity and rejection. Moreover, both autograft and cadaver-derived allografts present challenges such as the presence of inhibitory chondroitin sulfate proteoglycans, which reduce their performance as bridges and therefore require extra graft tissue processing (7, 8). Also, multiple lengths of nerve graft are often needed to bridge the gap between the injured nerve stumps. Ultimately, even with successful autografting, only 40% of patients regain useful function (9). Therefore, there is a clear, urgent, and

unmet clinical need for an alternative approach that can match or exceed autograft performance.

Given the myriad advances in the fields of regenerative medicine and materials engineering, many autograft alternatives have been explored (10–12). In both clinical and research settings, use of synthetic and natural guidance channels to bridge nerve gaps has been shown to improve nerve regeneration in small gaps (less than 10 mm in rat and 30 mm in human), but these constructs fail when the gaps are longer (11). Some tissue engineering strategies have shown promise, including the design of novel nerve conduits (3, 13), the addition of fillers within nerve conduits (14, 15), transplantation of cells (16, 17), local delivery of neurotrophic factors (18, 19), and application of topographical cues (20–22); however, none of these techniques has been able to match the autograft’s performance for long nerve gap repair (11, 12). Therefore, despite concerted effort over the last several decades, no suitable replacement for autografts has been found (3).

After PNS injuries, neurons respond rapidly by changing their activities and promoting a regenerative phenotype. At the distal nerve stump, Schwann cells (SCs) adopt a reparative phenotype. SCs, as well as infiltrating and resident macrophages, remove inhibitory debris, enabling new axons to sprout into the degenerated nerve directed by bands of Büngner (11). Although monocytes and their descendants (in particular, macrophages) have long been known to play an essential role in the degenerative process, only recently has their importance in positively influencing regeneration been recognized (23–26). Monocytes are abundant during nerve degeneration and regeneration and modulate the sequence of

## Significance

Annually, more than 250,000 Americans suffer from a peripheral nerve injury, which results in a loss of function and a compromised quality of life. The current clinical gold standard to bridge long, nonhealing nerve gaps, the autograft, has several drawbacks. Therefore, there is a clear and urgent unmet clinical need for an alternative approach that can match or exceed autograft performance. Here we investigated the regenerative effect of fractalkine, a chemokine that preferentially recruits reparative monocytes in the synthetic nerve conduit. Our method of bridging gaps enhanced axonal regeneration and muscle reinnervation and showed results comparable to those observed in autografts.

Author contributions: N.M., A.W.E., and R.V.B. designed research; N.M., K.D., A.S., and J.C. performed research; N.M., K.D., and A.S. contributed new reagents/analytic tools; N.M., J.G.L., J.T., A.W.E., and R.V.B. analyzed data; and N.M., J.G.L., J.T., A.W.E., and R.V.B. wrote the paper.

The authors declare no conflict of interest.

This article is a PNAS Direct Submission.

Freely available online through the PNAS open access option.

<sup>1</sup>To whom correspondence may be addressed. Email: [nassir.m@duke.edu](mailto:nassir.m@duke.edu) or [ravi@duke.edu](mailto:ravi@duke.edu).

This article contains supporting information online at [www.pnas.org/lookup/suppl/doi:10.1073/pnas.1705757114/-DCSupplemental](http://www.pnas.org/lookup/suppl/doi:10.1073/pnas.1705757114/-DCSupplemental).

cellular events which can determine the outcome of the healing process (24).

After inflammatory insult, macrophages that accumulate at the site of injury appear to be derived largely from circulating monocytes (27, 28); however, the precise kinetics and mechanisms of recruitment of blood monocyte populations to injured nerve tissues during normal repair remain to be elucidated (29, 30). The ability of monocytes to move to the site where they are needed is central to their function both in promoting immune defense and in tissue regeneration (29, 30). Entry of monocytes into the distal site of an injured nerve is enabled through up-regulation and release of a major monocyte chemokine, monocyte chemoattractant protein (CCL2) by SCs, which reaches its maximum 1 d after injury (31, 32). Besides CCL2, the CX3CR1 ligand (fractalkine) can also recruit monocytes through the CX3CR1 receptor (Fig. 1) (33, 34).

In rats, two major subsets of monocytes have been identified based on the expression of their chemokine receptors and CD43 levels (Fig. 1) (34–36): a CD43<sup>low</sup>CCR2<sup>+</sup>CX3CR1<sup>low</sup> inflammatory subtype of monocyte recruited to inflamed tissues and a CD43<sup>high</sup>CCR2<sup>-</sup>CX3CR1<sup>high</sup> antiinflammatory subtype (patrolling and reparative) recruited to healing tissues (36, 37). Inflammatory monocytes phagocytose debris and clear damaged cells, whereas antiinflammatory monocytes promote tissue regeneration (37). Even though the antiinflammatory monocytes are the larger population in rat blood under homeostatic conditions (80–90%), they constitute the smaller population in human blood (5–10%) (Fig. 1) (34).

These two subtypes of monocytes can be recruited to injured tissues, where they can subsequently differentiate into classically activated (M1) or alternatively activated (M2) macrophages (37). These two phenotypes of macrophages represent a simplistic discrete depiction of a continuous spectrum between two activation states (38). Generally, M1 macrophages produce proinflammatory cytokines as well as high levels of oxidative metabolites, and M2 macrophages make the environment supportive for tissue repair by producing antiinflammatory cytokines that facilitate matrix remodeling and angiogenesis (39, 40).

Although recruited monocytes differentiate to macrophages, recent studies have shown that monocytes also may have their own independent activities that are still to be elucidated (41, 42). For example, recent studies suggest that monocytes can promote arteriogenesis and angiogenesis (41), and thus they can act as short-lived effector cells within tissues (42). The mechanisms by which the antiinflammatory subset of monocytes/macrophages is either selectively recruited to or converted in situ at the site of peripheral nerve injury have not been investigated systematically (43).

The plasticity of monocytes/macrophages makes them an attractive target for modulation in the context of immunoengineering nerve repair. A prior short-term (3-wk) study demonstrated that direct modulation of macrophages toward a prohealing phenotype, using interleukin 4 (IL-4), results in an increase in SC recruitment and axonal growth (23). The premise herein is that preferential recruitment of antiinflammatory reparative monocytes to the site of

injury will more effectively bias the immune microenvironment toward a prohealing response and in turn set off a regenerative biochemical cascade involving SCs and neuronal processes that leads to improved repair (Fig. 2). Since CX3CR1 receptor is mainly expressed on antiinflammatory reparative monocytes (Fig. 1) (30, 34), exogenous fractalkine, the ligand for CX3CR1, can be used to preferentially recruit these monocytes to the site of nerve injury and thus increase the subsequent ratio of prohealing to proinflammatory macrophages during the regeneration process.

It has been shown that a marked increase in fractalkine mRNA was observed following facial nerve axotomy (44). In addition, the expression of the fractalkine receptor CX3CR1 in macrophages has been shown to increase not only in the sciatic nerve proximal to the site of injury but also in the dorsal root ganglion after the sciatic nerve section (axotomy) (45). Fractalkine administration after ischemic stroke also has been shown to increase neuronal survival and to contribute to angiogenesis through promotion of endothelial cell proliferation, thus leading to better functional recovery (46). Fractalkine does not bind to any known mammalian chemokine receptors except CX3CR1 and in fact is the only identified ligand to bind and activate the CX3CR1 receptor (47). Thus, the typical promiscuity that characterizes the chemokine superfamily is not present for fractalkine. This specificity suggests that the roles played by fractalkine and CX3CR1 are nonredundant and are critical for nerve regeneration (45).

This study investigated if local delivery of fractalkine within the lumen of a nerve conduit early after peripheral nerve injury led to enhanced nerve repair relative to IL-4-induced nerve repair (23) and traditional autografts.

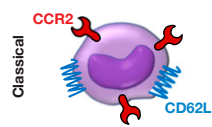

## Results

### Fractalkine Increases SC and Endothelial Cell Populations in Scaffolds.

A 15-mm gap model was constructed by grafting a transected nerve 1 mm into the ends of a 17-mm porous conduit filled with 1% (wt/vol) agarose hydrogel which was mixed with 10 µg/mL of either IL-4 or fractalkine (Fig. S1). We chose 1% agarose because of its structural properties that support axonal elongation (48). The IL-4 agarose scaffold was used as a benchmark because it has been shown previously to approach the regeneration potential of autografts (23, 26). The effect of short-term fractalkine delivery (<1 d release) (Fig. S2) on SCs (Fig. 3B) and endothelial cells (Fig. 3A) was investigated 4 wk after the conduit implantation. The 4-wk time point was the earliest among our previous studies that resulted in regenerated axons reaching the distal end of the 15-mm gap (23, 49). SCs and endothelial cells were studied to assess the effect of the therapeutics on changing the conduit environment's permissiveness for growth. As shown in Fig. 3, fractalkine delivery significantly increased both SC infiltration (determined by S100<sup>+</sup> staining) (Fig. 3D) and endothelial cells' migration [determined by rat endothelial cell antibody (RECA<sup>+</sup>) staining] (Fig. 3E) relative to the benchmark IL-4 control at this early time point (see Fig. S3 for higher-magnification images). It should be emphasized that the RECA staining used here is reactive only to vascular endothelium and does not react with other cells such as leukocytes, fibroblasts, and non-endothelial stromal cells.

### Fractalkine Improves the Ratio of Prohealing to Proinflammatory Macrophages.

There is an important correspondence between the number of regenerated axons and the profile of immune cells within the nerve conduit (23). As an indicator of the local immune state, the number and phenotype of macrophages were evaluated 4 wk after nerve conduit implantation using established markers (Figs. 4 and 5; see Fig. S3 for higher-magnification images) (21, 50–52). The number of macrophages at the distal end of the nerve conduit was significantly lower in the fractalkine scaffold than in the IL-4 scaffold (Fig. 4D). However, the number of prohealing macrophages (M2 macrophage subtypes M2a and M2c) as determined

	Main Marker	Percentage	Function
Classical			
	CD43 <sup>low</sup> (rat) CD14 <sup>high</sup> CD16 <sup>+</sup> (human)	~10–20% (rat) ~90–95% (human)	Inflammatory
Non-Classical			
	CD43 <sup>high</sup> (rat) CD14 <sup>low</sup> CD16 <sup>+</sup> (human)	~80–90% (rat) ~5–10% (human)	Patrolling/ Reparative

**Fig. 1.** Monocyte subtypes, receptors, markers, population percentage, and function.



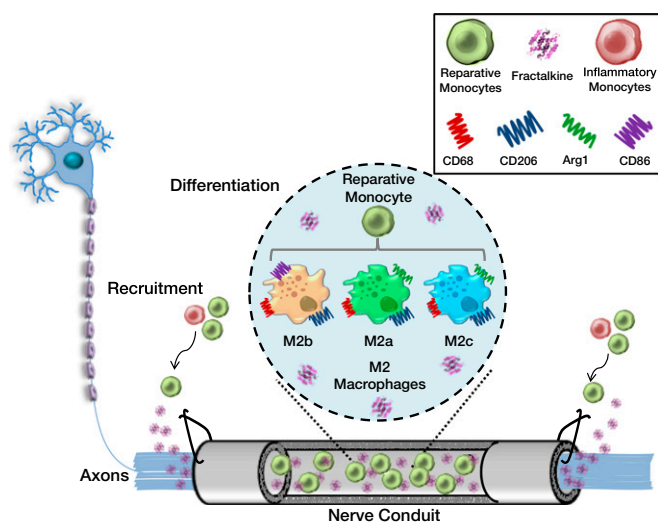


**Fig. 2.** Schematic for immunoen지니어링 nerve repair: recruitment and differentiation. This figure illustrates the response of circulating monocytes to the delivery of fractalkine at the site of nerve injury. A scaffold tube is sutured to the injured ends of the axotomized nerve and begins elution of fractalkine. Fractalkine recruits circulating monocytes, specifically reparative ones, to the site of injury, where further biochemical cues will potentially instruct the monocytes to differentiate into one of three potential prohealing macrophage phenotypes that enhance nerve repair:  $CD68^+CD206^+CD86^+$  (M2b) or  $CD68^+Arg1^+/CD206^+$  (M2a or M2c).

by  $CD68/Arginase$  costaining was not significantly different in these two conditions (Fig. 4E); therefore, the ratio of prohealing macrophages to the total number of macrophages (Fig. 4F) was significantly higher in the fractalkine scaffold than in the IL-4 scaffold. Also, the number and intensity of mannose receptors ( $CD206$ ), an antiinflammatory/wound-healing marker (Fig. 5B), were significantly higher in the fractalkine scaffold than in the IL-4 control (Fig. 5D). Furthermore, the number of  $CD206^+CD86^+$  cells (an indication of regulatory M2b macrophages) (Fig. 5C) was significantly higher in the fractalkine scaffold than in the control IL-4 scaffold (Fig. 5E). M2a and M2c macrophages appear during the early stage of healing process, whereas M2b macrophages, which have both pro- and antiinflammatory functions, can be induced toward the end of regeneration process (53).

Although Figs. 4B and 5B demonstrate the same trend of antiinflammatory markers, it is important to note that there is a subtle difference between the graphs in Figs. 4E and 5D; Fig. 4E represents the number of subset-specific macrophages (M2a and M2c) using costaining of arginase/ $CD68$  surface markers, while Fig. 5D portrays the number of all cells, not just macrophages, that have stained positive for the  $CD206$  surface marker.

**Fractalkine Dramatically Increases the Number of Regenerated Axons.** Axons at the distal end of the scaffold were visualized by immunostaining for neurofilament 160 (NF160) following nerve conduit explantation. Four weeks after implantation of the nerve conduit, the quantity of NF160 immunoreactive axons at the distal ends of the fractalkine scaffolds was significantly greater than in the IL-4-treated cohort (Fig. 6A and Fig. S4), i.e., nearly twice that found in the IL-4 scaffolds and very close to that observed in autografts (Fig. 6B). Although 1% agarose (SeaPrep) has been shown to be the optimal concentration to support axonal elongation (48), it had a detrimental effect on the distribution and homogeneity of regenerated axons at early time points, as evidenced by the lack of regeneration in the center of the nerve cable (Fig. S4). This detrimental effect has been observed in a previous study with an even lower concentration of agarose (26) and is believed to be related to the higher stiffness at the center of the hydrogel caused by cell-

mediated syneresis (54). Nevertheless, this central cavity is observed to be filled with regenerating axons at the later time points.

### Depletion of Monocytes Diminishes the Healing Effect of Fractalkine.

To investigate whether fractalkine's effect on nerve regeneration was mediated by its action on monocytes, clodronate liposome (CL-Lipo) treatment, a well-established methodology to deplete circulating monocytes and subsequently the number of infiltrating macrophages at the site of injury (55–57), was used. Animals were injected with CL-Lipo once, 48 h before nerve conduit implantation. Rats with fractalkine scaffolds with CL-Lipo injection were compared with rats with fractalkine scaffold with sham PBS injections. As shown in Fig. 7, depleting circulating monocytes and consequently infiltrating macrophages during the release of fractalkine from the nerve conduit (Fig. S2) (23) diminishes the axonal growth-stimulating effect of fractalkine (Fig. 7A). After 10 d, the advance of axons toward the distal end of the conduit in the macrophage/monocyte-depleted samples was limited largely to the proximal stump of the conduit, less than 2 mm from the initial placement of the transected nerve sutured within the nerve conduit (Fig. 7B). On the other hand, the average axonal growth within the fractalkine nerve conduits in sham-injected animals was considerably longer than in CL-Lipo-injected animals (4.5 mm growth considering its initial positioning at 1 mm inside the conduit) (Fig. 7B).

### Electrophysiological Analyses Indicates Muscle Reinnervation Caused by Fractalkine.

Because of the superior regeneration with fractalkine delivery relative to IL-4 delivery, a longer-term (14-wk) study was undertaken to evaluate relative functional recovery after fractalkine or autograft intervention in critically sized nerve gaps with a negative control (nerve conduit filled with 1% agarose without any immunomodulatory factor) (Fig. S5).

Two electromyographic (EMG) potentials were recorded in response to sciatic nerve stimulation: a short-latency direct muscle response (M-wave) produced by stimulating motor axons and a slightly longer latency reflex (H-reflex) produced by activating motoneurons synaptically via stimulation of sensory axons in the sciatic

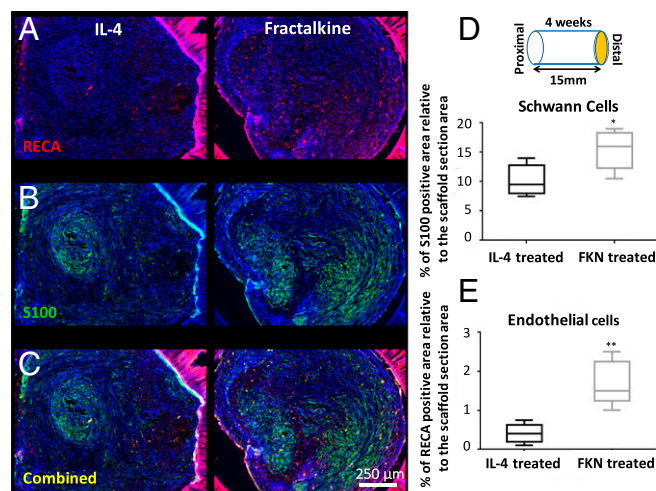


**Fig. 3.** The effect of early fractalkine release on SCs and endothelial cells. (A) Combined RECA (red), and DAPI (blue) staining. (B) Combined S100 (green) and DAPI (blue) staining. (C) Combined S100 (green), RECA (red), and DAPI (blue) staining. (D) Quantitative analysis of  $S100^+$  staining of SCs at the distal end of the conduit ( $P = 0.0243$ , two-tailed  $t$  test). (E) Quantitative analysis of RECA $^+$  staining of endothelial cells at the distal end of the conduit ( $P = 0.0016$ , two-tailed  $t$  test) ( $n = 5$ ). The fractalkine-treated scaffold significantly enhanced both SC infiltration and endothelial cell presence inside the nerve conduit in comparison with the IL-4-treated scaffold 4 wk after implantation. FKN, fractalkine.

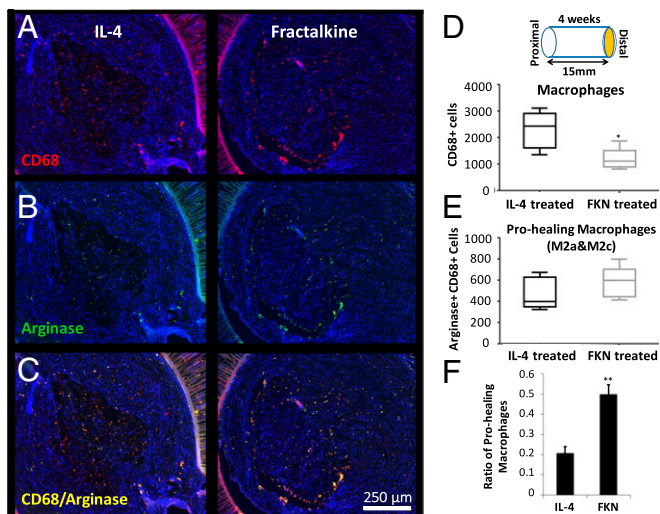


**Fig. 4.** The effect of early fractalkine release on the number and phenotype of macrophages. (A) Combined CD68 (red), and DAPI (blue) staining. (B) Combined arginase (green) and DAPI (blue) staining. (C) Combined arginase (green), CD68 (red), and DAPI (blue) staining. (D) Quantitative analysis of total macrophage numbers at the distal end by using the CD68 marker ( $P = 0.015$ , two-tailed  $t$  test). (E) Quantitative analysis of prohealing macrophages at the distal end by double staining with CD68 and arginase ( $P = 0.288$ , two-tailed  $t$  test). (F) The ratio of prohealing macrophages to the total number of macrophages ( $P = 0.0019$ ) ( $n = 5$ ). Four weeks after implantation the fractalkine-treated scaffold has significantly fewer macrophages but a higher ratio of prohealing macrophage than the IL-4-treated scaffold. This figure is reproduced in part from ref. 66. FKN, fractalkine.

nerve. By scaling the maximum amplitude of the M-wave (M Max) in reinnervated gastrocnemius muscles to the corresponding measures from the intact contralateral gastrocnemius muscles, the relative effectiveness of axon regeneration and muscle reinnervation in the different treatment groups could be compared (Fig. 8). When scaled to the corresponding contralateral EMG signals, the M Max median was larger in autografted rats (0.73) than in those with fractalkine conduits (0.58), and both were larger than in the control group (0.04) (Fig. 8B). Although there were significant differences between these scaled M Max amplitudes in autograft and control rats ( $P < 0.001$ ) and between the fractalkine and control rats ( $P < 0.01$ ), there was no statistically significant difference between the autograft and fractalkine groups (Fig. 8B). In contrast, the difference in the scaled maximum H-reflex amplitudes (H Max) between the autograft and fractalkine groups is statistically significant ( $P < 0.01$ ) (Fig. 8C). The medians of H Max (scaled to the contralateral side) for the autograft, fractalkine, and control groups were 0.55, 0.15, and 0.02, respectively (Fig. 8C). No statistically significant differences in latency to the start of the EMG response were found between the fractalkine and the autograft groups (Fig. 8D).

The ratio of H Max to M Max was also studied for these groups of animals. This ratio represents a measure of the extent of recruitment of all motoneurons whose axons have successfully reinnervated the gastrocnemius muscle into the H-reflex. In self-reinnervated muscle, this ratio is only about half as large (59%) as in intact muscle (58). Because a majority of negative control conduits did not show any positive M or H response, the magnitude of the H Max/M Max ratio measured from reinnervated muscles was analyzed and reported only in the autograft and fractalkine groups (Fig. 8E). Rats in the fractalkine group had a significantly higher scaled H Max/M Max ratio than animals in the autograft group ( $P < 0.05$ ) (Fig. 8E). The median H Max/M Max ratios for the autograft and fractalkine groups are 0.14 and 0.40, respectively, indicating that the efficacy of this reflex is restored more in the fractalkine group than in the autograft group.

Last, the H and M response duration in autograft and fractalkine groups were compared (Fig. S6). No significant difference was observed in the latency profiles of these two groups (Fig. S6); however, the absence of significant differences among the groups may be a result of the inherent difficulty in quantifying this measure accurately (see *Supporting Information* for more detail).

**Histological Analyses at 14 wk Further Indicate Enhanced Nerve Regeneration Caused by Fractalkine.** To support our functional analyses with anatomical data, additional histological analyses were performed at the 14-wk time point (Fig. 9A and B and Fig. S7). Along with a standard axonal count, myelin thickness and myelinated axon density were measured. Despite the very different spatial appearance of the regenerating axons in the autograft and fractalkine groups, there was no significant difference in the mean numbers of regenerating axons in these two groups (Fig. S7). The numbers of myelinated axons at the distal ends of scaffolds were significantly higher in both the autograft ( $7,736 \pm 1,136$ ) and fractalkine ( $6,131 \pm 2,078$ ) groups than in the control ( $342 \pm 363$ ) group ( $P < 0.0001$ ). However, the distribution of regenerated axons was significantly distinct in the different groups and was most homogeneous in the autograft group (Fig. S7). The myelinated axon density in the tissue-positive regions of nerve cable was also significantly larger in the autograft ( $3.29 \pm 0.53$  E-2 axons/ $\mu\text{m}^2$ ) and fractalkine ( $3.88 \pm 0.61$  E-2 axons/ $\mu\text{m}^2$ ) groups than in the control ( $8.66 \pm 13.6$  E-4 axons/ $\mu\text{m}^2$ ) group ( $P < 0.0001$ ), but the differences observed between the autograft and fractalkine groups were not significant (Fig. 9C). The average thickness of myelin in the autograft group ( $1.547 \pm 0.04$   $\mu\text{m}$ ) was greater than that found in sections in the fractalkine group ( $1.385 \pm 0.09$   $\mu\text{m}$ ), but these differences were not significant (Fig. 9D).

## Discussion

Autografts are the current standard for bridging long peripheral nerve gaps, but several drawbacks limit their use. Currently, as an

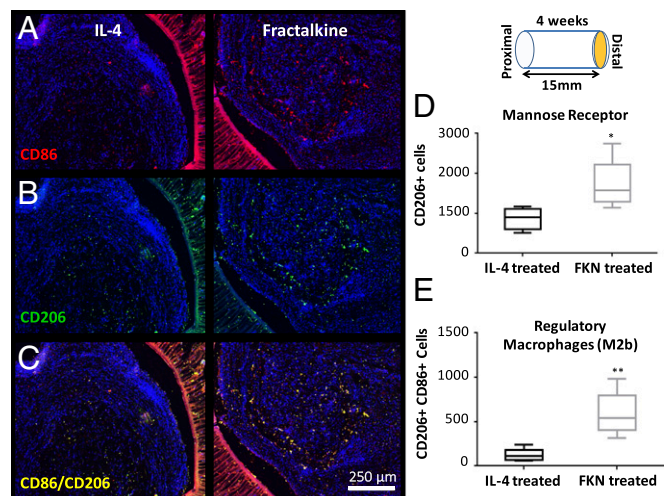


**Fig. 5.** The effect of early fractalkine release on mannose receptor expression and regulatory macrophages. (A) Combined CD86 (red) and DAPI (blue) staining. (B) Combined CD206 (green) and DAPI (blue) staining. (C) Combined CD86 (red), CD206 (green), and DAPI (blue) staining. (D) Quantitative analysis of mannose receptor-expressing cells at the distal end assessed by the marker CD206 ( $P = 0.022$ , two-tailed  $t$  test). (E) Quantitative analysis of regulatory macrophages (M2b) at the distal end by double staining with CD86 and mannose receptor ( $P = 0.003$ , two-tailed  $t$  test) ( $n = 5$ ). Four weeks after implantation, the fractalkine-treated scaffold contains a higher number of mannose receptor-expressing cells and regulatory macrophages than the IL-4-treated scaffold. FKN, fractalkine.



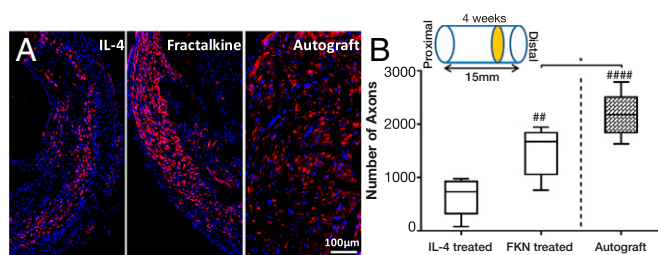


**Fig. 6.** The effect of fractalkine release on axonal growth. (A) Immunohistochemical staining of axons (red) and DAPI (blue) at the distal end of nerve stump. (B) The number of regenerated axons at the distal end of the fractalkine- vs. the IL-4-treated scaffold in comparison with the autograft 4 wk after injury. \* $P < 0.05$ ; ## $P < 0.01$ ; ### $P < 0.0001$  (one-way ANOVA) ( $n = 5$ ). Fractalkine-treated scaffold dramatically increases the number of regenerated axons relative to IL-4, reaching very close to the number of regenerated axons in autograft.

alternative to autografts, synthetic biomaterial-based nerve conduits have been developed that are capable of bridging short gaps (11, 13, 21, 59, 60). However, these nerve conduits have not been very successful in bridging critically sized nerve gaps. Subsequently, functional recovery is rarely achieved in those gaps (11). The approach in this study was to enhance nerve regeneration across long gaps by preferentially recruiting a subset of reparative monocytes to the site of injury (Fig. 2).

In this study, we show that fractalkine, as compared with IL-4, significantly enhances the ratio of prohealing macrophages to the total number of macrophages 4 wk after scaffold implantation (Fig. 4F) even though the number of macrophages is lower in the fractalkine scaffolds than in the IL-4 scaffolds (Fig. 4D). We have previously demonstrated the direct correlation between the ratio of prohealing macrophages and the number of regenerated axons (23). The results of this study confirm that the phenotype of macrophages, and not their number, correlates with the regeneration outcome in the later stages of nerve repair. It is believed that, when the difference in the number of macrophages is not substantial, the ratio of prohealing to proinflammatory macrophages determines the permissiveness of the conduit environment for growth (23, 26). The criterion for permissiveness used was the quantity of infiltrated SCs and endothelial cells in the conduits a few weeks after implantation (Fig. 3 A–C). Based on this criterion, the fractalkine scaffold outperformed the IL-4 scaffold significantly (Fig. 3 D and E).

Given the data presented here, it is clear that scaffolds containing fractalkine result in a dramatically higher number of axons at the distal end of the nerve conduit than scaffolds containing IL-4 (Fig. 6). Further, it was confirmed that the reparative effect of fractalkine was enabled through monocyte/macrophages because systematic depletion of monocytes from the blood with CL-Lipo during fractalkine release inside the nerve conduit diminished the positive reparative effect of fractalkine (Fig. 7). Hence, this study strongly highlights the important role that monocytes and macrophages play during the nerve regeneration process enhanced by fractalkine. Moreover, because fractalkine recruits CX3CR1<sup>+</sup> monocytes (33), which include only reparative monocytes in rats (34), the regenerative effect of fractalkine seems to occur via the contribution of this monocyte subtype.

The extent of axon regeneration and muscle reinnervation in different treatment groups was studied by analyzing different characteristics of the M-wave and H-reflex responses elicited by stimulus to the sciatic nerve and recorded in the gastrocnemius muscle. As described by Palmieri, et al. (61), the measurement of H Max and M Max provides a valuable tool for the evaluation of nerve health in clinical diagnostic use. Similarly, these values can be used to evaluate the success of healthy reinnervation. Eight weeks after injury, a chronically denervated distal stump loses its capability to support axonal growth, and after 6 mo the stump

becomes completely incapable of supporting reinnervation (62). It is critical for axons to reach their target muscle during this 8-wk to 6-mo regenerative time window (62, 63). Therefore, our electrophysiological analyses of affected nerve/muscle (sciatic nerve/gastrocnemius muscle) were conducted 14 wk after the nerve transection.

The nearly complete return of the H Max/M Max ratio to pre-transection values in rats from our fractalkine-treated group is one of the more striking findings of this study. The H Max/M Max ratio represents a measure of the extent of recruitment of all motoneurons whose axons have successfully reinnervated the gastrocnemius muscle into the H-reflex. In 10 intact, healthy rats the average H Max/M Max ratio ( $\pm$  SEM) was 0.44 (0.069) (64). In sciatic nerve transections repaired using the fractalkine scaffold, the mean H Max/M Max ratio was 0.40 (Fig. 8E), a value of 91% when scaled to the Hmax/Mmax ratio found in intact rats. This H Max/M Max ratio was more than twice that observed in autograft-treated rats (Fig. 8E) and even higher than in rats with cut sciatic nerves that had been repaired by end-to-end anastomosis (64). We interpret these findings as evidence that the fractalkine treatments influenced the regeneration not only of motor and sensory axons in the periphery but also of circuitry in the spinal cord.

The scaled M Max values were significantly greater in rats in which sciatic nerve transections were repaired using either autografts or scaffolds containing the fractalkine protein than in rats with transections repaired with the control scaffolds filled only by agarose hydrogel (Fig. 8B). Late-time-point histological analyses also corroborate the electrophysiological findings about the overall quality of the regenerative nerve cable (Fig. 9 and Fig. S7). We interpret these data to mean that motor axon regeneration was enhanced significantly in both the autograft and fractalkine groups. Because differences in M-wave amplitudes in the autograft and fractalkine groups were not significant, we conclude that our fractalkine-treated scaffolds represent a synthetic alternative that closely matched an important aspect of autograft electrophysiological performance, the M-wave response. It is important to recall that the autograft contains SCs, whereas the fractalkine group recruits endogenous cells and does not have any autogenic transplants similar to the autograft. It is

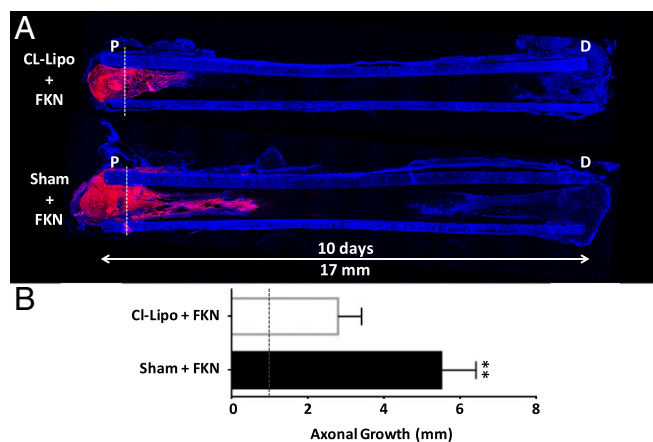


**Fig. 7.** CL-Lipo study. (A) Axonal regeneration (stained red with NF160 antibody) is demonstrated using longitudinally sectioned scaffolds in the CL-Lipo-treated animal vs. the nontreated animal ( $n = 4$ ). Both scaffolds contain fractalkine. (B) Quantification of the length of axonal growth 10 d after scaffold implantation ( $P = 0.003$ , two-tailed  $t$  test). Dotted line in both A and B indicates the position of nerve on day 0. Partial depletion of monocytes using a single injection of CL-Lipo 48 h before nerve conduit implantation significantly reduces the amount of axonal growth, indicating the central role that monocyte presence plays in the fractalkine-treated scaffold (blue = DAPI). This image is reproduced in part from ref. 66. FKN, fractalkine.

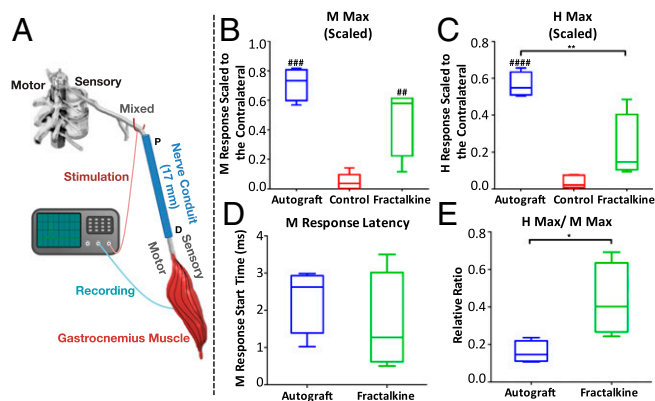


**Fig. 8.** Electrophysiological analysis. (A) Schematic demonstrating proximal stimulation of sciatic nerve motor axons and recording of the EMG signal from reinnervated gastrocnemius muscle 14 wk after scaffold implantation. (B and C) M Max (B) and H Max (C) amplitudes in the autograft group vs. the control scaffold and the fractalkine-loaded scaffold groups. (D and E) M-response latency (D) and H Max/M Max ratio (E) in the autograft vs. the fractalkine-loaded scaffold groups. \* $P < 0.05$ ; ## $P < 0.01$ ; ### $P < 0.001$ ; #### $P < 0.0001$  (one-way ANOVA or two-tailed *t* test) ( $n = 6$ ). M Max in rats with the fractalkine-loaded scaffold is significantly larger than in control rats and very closely approaches the autograft performance. H Max in rats with the fractalkine-loaded scaffold is still significantly lower than autograft, whereas the H Max/M Max ratio in rats with the fractalkine-loaded scaffold is significantly larger than autograft.

also important to note that in this nerve gap an agarose-only nerve-guidance channel elicits no axon regeneration, because the experimental model is a critically sized gap.

Across almost all late-time-point measures, greater data variability was observed among the groups of rats that had the sciatic nerve repaired using the scaffold, and especially fractalkine treatment, than in the autograft group. This variability can be explained by the inherent differences in each animal's monocyte recruitment response; also, in this kind of extremely early intervention, small changes in the efficacy could result in big changes in outcome. For example, the effects of small differences in early monocyte recruitment may be amplified by other players in the cascade of regeneration such as macrophages, fibroblasts, endothelial cells, and SCs (12).

Although early engagement of macrophages and their consequent state of activation play critical roles in determining the fate of the healing process (23, 55, 65), the underlying mechanism whereby short-lived fractalkine treatment provides a sustained increase in reparative macrophages and subsequently dramatically better healing remains unclear. Additionally, the particular role of fractalkine and its receptor in the accumulation of monocytes and macrophages at injured peripheral nerves has not been elucidated. Unraveling the process of monocyte recruitment after peripheral nerve injuries could provide further insights for the development of new therapeutics based on manipulating the number and distribution of these cells as a way to enhance the proregenerative immune response (30).

## Conclusion

Current treatment options available for patients with peripheral nerve injury are unsatisfactory. Off-the-shelf availability of long synthetic grafts would revolutionize the acute management of complex peripheral nerve injuries, allowing surgeons to bridge multiple nerves immediately at the time of injury. The innovative approach described here uses the endogenous capacity of the body for healing using its own innate immune cells. In contrast to the current established views regarding tissue remodeling and inflammation, strategies that promote the temporal, spatial, and

phenotypical recruitment of monocytes can encourage the functional recovery of damaged tissue instead of exacerbating injury.

The data presented in this study suggest that the release of an antiinflammatory monocyte-recruiting factor, fractalkine, early after nerve injury can dramatically enhance the permissiveness of nerve conduits, stimulate axonal growth 4 wk after axotomy, and enhance electrophysiological outcomes at 14 wk. Controlling monocyte subtype recruitment, rather than preventing monocyte infiltration to the injured tissue, is a functional shift in tissue engineering approaches. The data from this study clearly attest to the effectiveness of this immunoen지니어ing approach to nerve repair.

## Materials and Methods

**Scaffold Implantation.** Polysulfone tubes filled with 1% agarose (SeaPrep Lonza) mixed with 10  $\mu\text{g}/\text{mL}$  rat recombinant chemokine fractalkine or IL-4 (Antigenix America, Inc.) or with agarose only were prepared ( $n = 13$  per group) (Fig. S1). We chose 1% SeaPrep agarose because its mechanical properties and porosity had been demonstrated previously as being supportive of axonal growth as well as ensuring the complete filling of the scaffold to achieve uniform short-term release of cytokine (Fig. S2) (48). Microscissors were used to transect the sciatic nerve, and the nerve stumps were pulled 1 mm into each end of the 17-mm-long guidance scaffolds (leaving a 15-mm gap) and were fixed in place with a single 10-0 nylon suture (Ethicon). As a positive control, using a standard protocol (21), we created nerve autografts in some rats by resecting a segment of rat sciatic nerve and then flipping it to bridge the 15-mm gap ( $n = 8$ ). Animals were maintained in facilities approved by the Institutional Animal Care and Use Committee (IACUC) at the Georgia Institute of Technology or Emory University and in accordance with the US Department of Agriculture, US Department of Health and Human Services, and NIH regulations and standards. IACUC at the aforementioned universities also approved all the protocols for research involving animal subjects. For details see *SI Text*.

**CL-Lipo Study.** The CL-Lipo suspension was purchased from Clodronate Liposomes. To prevent precipitation of liposomes, the suspension was shaken before injection. A homogeneous suspension was required to warrant an equal concentration of liposomes per milliliter. For i.v. injection, 0.1 mL of the suspension was injected per 10 g of animal weight 48 h before the implantation. Depletion of liver and splenic macrophages was complete after

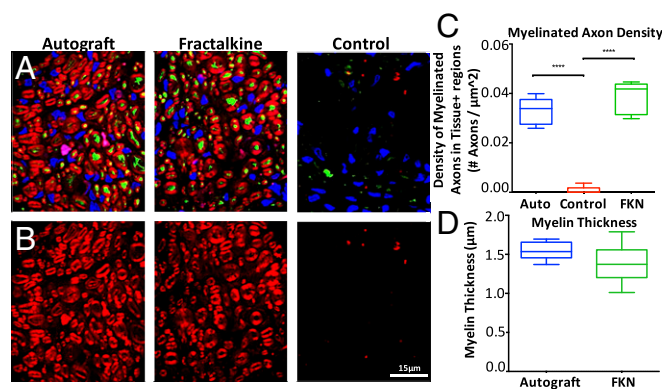


**Fig. 9.** Histological analysis of myelin and axon density at the late time point. (A) Representative pseudocolored fluorescent images showing NF160 (green), FluoroMyelin (red), and DAPI (blue) staining of scaffold cross-sections for autograft, fractalkine, and control groups. (B) Representative pseudocolored fluorescent images showing FluoroMyelin (red) staining of scaffold cross-sections at the 14-wk time point for autograft, fractalkine, and control groups, respectively. (C) Density of myelinated axons (normalized to the combined area of tissues positively stained for any of NF160, FluoroMyelin, or DAPI, not to the total image area) comparing autograft, fractalkine, and control ( $n = 8$ ). The densities in the autograft and fractalkine groups are not significantly different, but both are significantly higher than in the control group (\*\*\*\* $P < 0.0001$ ). (D) Comparison of myelin thickness surrounding regenerated axons in autograft and fractalkine ( $n = 8$ ). The average thickness of myelin is greater in the autograft group than in the fractalkine group, but these differences are not statistically significant. FKN, fractalkine.

~24 h. Two experimental groups were included ( $n = 4$ ): fractalkine scaffolds with CL-Lipo injection, and fractalkine scaffolds with sham PBS injection (see *SI Text* for more details). Scaffolds were explanted for analysis 10 d postimplantation.

**Scaffold Explantation and Histological Analysis.** Unless otherwise stated, scaffolds or autografts were explanted at 4 wk or 14 wk postimplantation for histological analysis of nerve regeneration ( $n = 5$  or 8). Because axons grow from the proximal to the distal end of the scaffold, and the Wallerian degeneration process mainly affects the distal end of the nerve (26), the last 2 mm of the distal end was used for histological analysis. Nerve tissue was sectioned from the distal end (where the scaffold started or at the distal autograft suture mark), and three sections were collected every 200  $\mu\text{m}$ . Suture marks on the nerve or nerve scaffold were used to choose spatially consistent and comparable sections. The remaining parts of scaffolds or autografts were snap-frozen in liquid nitrogen and stored at  $-80^\circ\text{C}$  for further analysis. Explants were fixed in 4% paraformaldehyde (Sigma Aldrich), washed, and stored in 30% sucrose for 24 h. Samples were embedded in optimum cutting temperature gel (Tissue-Tek) and frozen for cryosectioning (CM3050S; Leica). Autografts or scaffolds were sectioned transversely or longitudinally to a thickness of 16  $\mu\text{m}$  and reacted with immunofluorescent markers to quantify the different cell types, using techniques previously described (21) and as explained further in *SI Text*.

**Electrophysiology.** Axon regeneration and muscle fiber reinnervation were studied using evoked EMG activity in ketamine/xylazine-anesthetized animals at 14 wk posttransection (for details see *SI Text*, Fig. S8). The sciatic nerve was stimulated on each side of the animal in the midhigh, proximal to the surgical repair site on the injured side of the animal, and direct muscle (M-wave) and monosynaptic H-reflexes were recorded from the gastrocnemius muscle. The largest M-wave and H-reflex and their ratio were recorded, and responses on the injured side of each rat were scaled to the corresponding responses on the intact side. Autograft-, fractalkine-, and control sham-treated cohorts ( $n = 6$ ) were compared. For more information, please refer to *SI Text*.

**Statistical Analysis.** To determine significant differences among groups, data were analyzed using Prism 6 (GraphPad) with an unpaired Student's  $t$  test for two-group comparisons and one-way ANOVA with pairwise Tukey's multiple comparison test for data with more than two groups. A  $P$  value  $<0.05$  was defined to indicate a statistically significant difference. Data are reported as mean  $\pm$  SD unless otherwise specified.

**ACKNOWLEDGMENTS.** We thank Dr. Balakrishna Pai and Dr. Tarun Saxena for helpful scientific and editorial discussions; Sohee Park, Yogi Patel, and Sheridan Carroll for their technical support on electrophysiological and imaging analyses; and Dr. Giles W. Plant for his suggestions regarding myelin staining. This work was supported by NIH Grants 7R01NS093666 and 5R01NS065109.

- Belkas JS, Shoichet MS, Midha R (2004) Peripheral nerve regeneration through guidance tubes. *Neural Res* 26:151–160.
- Millesi H (2006) Factors affecting the outcome of peripheral nerve surgery. *Microsurgery* 26:295–302.
- Bellamkonda RV (2006) Peripheral nerve regeneration: An opinion on channels, scaffolds and anisotropy. *Biomaterials* 27:3515–3518.
- Giusti G, et al. (2012) Return of motor function after segmental nerve loss in a rat model: Comparison of autogenous nerve graft, collagen conduit, and processed allograft (AxoGen). *J Bone Joint Surg Am* 94:410–417.
- Wood MD, et al. (2014) Rat-derived processed nerve allografts support more axon regeneration in rat than human-derived processed nerve xenografts. *J Biomed Mater Res A* 102:1085–1091.
- Szynkaruk M, Kemp SWP, Wood MD, Gordon T, Borschel GH (2013) Experimental and clinical evidence for use of decellularized nerve allografts in peripheral nerve gap reconstruction. *Tissue Eng Part B Rev* 19:83–96.
- Zuo J, Hernandez YJ, Muir D (1998) Chondroitin sulfate proteoglycan with neurite-inhibiting activity is up-regulated following peripheral nerve injury. *J Neurobiol* 34:41–54.
- Groves ML, et al. (2005) Axon regeneration in peripheral nerves is enhanced by proteoglycan degradation. *Exp Neurol* 195:278–292.
- Lee SK, Wolfe SW (2000) Peripheral nerve injury and repair. *J Am Acad Orthop Surg* 8:243–252.
- Pfister BJ, et al. (2011) Biomedical engineering strategies for peripheral nerve repair: Surgical applications, state of the art, and future challenges. *Crit Rev Biomed Eng* 39:81–124.
- Mukhatyar V, Karumbaiah L, Yeh J, Bellamkonda R (2009) Tissue engineering strategies designed to realize the endogenous regenerative potential of peripheral nerves. *Adv Mater* 21:4670–4679.
- Mokarram N, Bellamkonda RV (2011) Overcoming endogenous constraints on neuronal regeneration. *IEEE Trans Biomed Eng* 58:1900–1906.
- Dodla MC, Bellamkonda RV (2008) Differences between the effect of anisotropic and isotropic laminin and nerve growth factor presenting scaffolds on nerve regeneration across long peripheral nerve gaps. *Biomaterials* 29:33–46.
- Madaghiele M, Sannino A, Yannas IV, Spector M (2008) Collagen-based matrices with axially oriented pores. *J Biomed Mater Res A* 85:757–767.
- Chamberlain LJ, Yannas IV, Hsu HP, Spector M (2000) Connective tissue response to tubular implants for peripheral nerve regeneration: The role of myofibroblasts. *J Comp Neurol* 417:415–430.
- Rodríguez FJ, Verdú E, Ceballos D, Navarro X (2000) Nerve guides seeded with autologous schwann cells improve nerve regeneration. *Exp Neurol* 161:571–584.
- Nie X, et al. (2007) Improvement of peripheral nerve regeneration by a tissue-engineered nerve filled with ectomesenchymal stem cells. *Int J Oral Maxillofac Surg* 36:32–38.
- Fine EG, Decosterd I, Papaloizos M, Zurn AD, Aebischer P (2002) GDNF and NGF released by synthetic guidance channels support sciatic nerve regeneration across a long gap. *Eur J Neurosci* 15:589–601.
- Lee AC, et al. (2003) Controlled release of nerve growth factor enhances sciatic nerve regeneration. *Exp Neurol* 184:295–303.
- Hoffman-Kim D, Mitchell JA, Bellamkonda RV (2010) Topography, cell response, and nerve regeneration. *Annu Rev Biomed Eng* 12:203–231.
- Kim Y-T, Haftel VK, Kumar S, Bellamkonda RV (2008) The role of aligned polymer fiber-based constructs in the bridging of long peripheral nerve gaps. *Biomaterials* 29:3117–3127.
- Spivey EC, Khaing ZZ, Shear JB, Schmidt CE (2012) The fundamental role of subcellular topography in peripheral nerve repair therapies. *Biomaterials* 33:4264–4276.
- Mokarram N, Merchant A, Mukhatyar V, Patel G, Bellamkonda RV (2012) Effect of modulating macrophage phenotype on peripheral nerve repair. *Biomaterials* 33:8793–8801.
- Gaudet AD, Popovich PG, Ramer MS (2011) Wallerian degeneration: Gaining perspective on inflammatory events after peripheral nerve injury. *J Neuroinflammation* 8:110.
- DeFrancesco-Lisowitz A, Lindborg JA, Niemi JP, Zigmund RE (2015) The neuro-immunology of degeneration and regeneration in the peripheral nervous system. *Neuroscience* 302:174–203.
- Mokarram N, Bellamkonda RV (2014) A perspective on immunomodulation and tissue repair. *Ann Biomed Eng* 42:338–351.
- Cortez-Retamozo V, Etzrodt M, Pittet MJ (2012) Regulation of macrophage and dendritic cell responses by their lineage precursors. *J Innate Immun* 4:411–423.
- Yona S, Jung S (2010) Monocytes: Subsets, origins, fates and functions. *Curr Opin Hematol* 17:53–59.
- Bellingan GJ, et al. (2002) Adhesion molecule-dependent mechanisms regulate the rate of macrophage clearance during the resolution of peritoneal inflammation. *J Exp Med* 196:1515–1521.
- Shi C, Pamer EG (2011) Monocyte recruitment during infection and inflammation. *Nat Rev Immunol* 11:762–774.
- Perrin FE, Lacroix S, Avilés-Trigueros M, David S (2005) Involvement of monocyte chemoattractant protein-1, macrophage inflammatory protein-1 $\alpha$  and interleukin-1 $\beta$  in Wallerian degeneration. *Brain* 128:854–866.
- Toews AD, Barrett C, Morell P (1998) Monocyte chemoattractant protein 1 is responsible for macrophage recruitment following injury to sciatic nerve. *J Neurosci Res* 53:260–267.
- Chapman GA, et al. (2000) The role of fractalkine in the recruitment of monocytes to the endothelium. *Eur J Pharmacol* 392:189–195.
- Strauss-Ayali D, Conrad SM, Mosser DM (2007) Monocyte subpopulations and their differentiation patterns during infection. *J Leukoc Biol* 82:244–252.
- Ahuja V, Miller SE, Howell DN (1995) Identification of two subpopulations of rat monocytes expressing disparate molecular forms and quantities of CD43. *Cell Immunol* 163:59–69.
- Gordon S, Taylor PR (2005) Monocyte and macrophage heterogeneity. *Nat Rev Immunol* 5:953–964.
- Awojoodu AO, et al. (2013) Sphingosine 1-phosphate receptor 3 regulates recruitment of anti-inflammatory monocytes to microvessels during implant arteriogenesis. *Proc Natl Acad Sci USA* 110:13785–13790.
- Mosser DM, Edwards JP (2008) Exploring the full spectrum of macrophage activation. *Nat Rev Immunol* 8:958–969.
- Edwards JP, Zhang X, Frauwirth KA, Mosser DM (2006) Biochemical and functional characterization of three activated macrophage populations. *J Leukoc Biol* 80:1298–1307.
- Gordon S, Martinez FO (2010) Alternative activation of macrophages: Mechanism and functions. *Immunity* 32:593–604.
- Avraham-David I, et al. (2013) On-site education of VEGF-recruited monocytes improves their performance as angiogenic and arteriogenic accessory cells. *J Exp Med* 210:2611–2625.
- Jakubzick C, et al. (2013) Minimal differentiation of classical monocytes as they survey steady-state tissues and transport antigen to lymph nodes. *Immunity* 39:599–610.
- Novak ML, Koh TJ (2013) Phenotypic transitions of macrophages orchestrate tissue repair. *Am J Pathol* 183:1352–1363.
- Harrison JK, et al. (1998) Role for neuronally derived fractalkine in mediating interactions between neurons and CX3CR1-expressing microglia. *Proc Natl Acad Sci USA* 95:10896–10901.
- Holmes FE, et al. (2008) Intra-neural administration of fractalkine attenuates neuropathic pain-related behaviour. *J Neurochem* 106:640–649.



46. Qin W, et al. (2014) Exogenous fractalkine enhances proliferation of endothelial cells, promotes migration of endothelial progenitor cells and improves neurological deficits in a rat model of ischemic stroke. *Neurosci Lett* 569:80–84.
47. Stievano L, Piovan E, Amadori A (2004) C and CX3C chemokines: Cell sources and physiopathological implications. *Crit Rev Immunol* 24:205–228.
48. Dillon GP, Yu X, Sridharan A, Ranieri JP, Bellamkonda RV (1998) The influence of physical structure and charge on neurite extension in a 3D hydrogel scaffold. *J Biomater Sci Polym Ed* 9:1049–1069.
49. Clements IP, et al. (2009) Thin-film enhanced nerve guidance channels for peripheral nerve repair. *Biomaterials* 30:3834–3846.
50. Brown BN, Valentin JE, Stewart-Akers AM, McCabe GP, Badyrak SF (2009) Macrophage phenotype and remodeling outcomes in response to biologic scaffolds with and without a cellular component. *Biomaterials* 30:1482–1491.
51. Brown BN, et al. (2012) Macrophage phenotype as a predictor of constructive remodeling following the implantation of biologically derived surgical mesh materials. *Acta Biomater* 8:978–987.
52. Badyrak SF, Valentin JE, Ravindra AK, McCabe GP, Stewart-Akers AM (2008) Macrophage phenotype as a determinant of biologic scaffold remodeling. *Tissue Eng Part A* 14:1835–1842.
53. David S, Kroner A (2011) Repertoire of microglial and macrophage responses after spinal cord injury. *Nat Rev Neurosci* 12:388–399.
54. Balgude AP, Yu X, Szymanski A, Bellamkonda RV (2001) Agarose gel stiffness determines rate of DRG neurite extension in 3D cultures. *Biomaterials* 22:1077–1084.
55. Godwin JW, Pinto AR, Rosenthal NA (2013) Macrophages are required for adult salamander limb regeneration. *Proc Natl Acad Sci USA* 110:9415–9420.
56. Summan M, et al. (2006) Macrophages and skeletal muscle regeneration: A clodronate-containing liposome depletion study. *Am J Physiol Regul Integr Comp Physiol* 290:R1488–R1495.
57. Valentin JE, Stewart-Akers AM, Gilbert TW, Badyrak SF (2009) Macrophage participation in the degradation and remodeling of extracellular matrix scaffolds. *Tissue Eng Part A* 15:1687–1694.
58. English AW, Chen Y, Carp JS, Wolpaw JR, Chen XY (2007) Recovery of electromyographic activity after transection and surgical repair of the rat sciatic nerve. *J Neurophysiol* 97:1127–1134.
59. Taras JS, Nanavati V, Steelman P (2005) Nerve conduits. *J Hand Ther* 18:191–197.
60. Siemionow M, Bozkurt M, Zor F (2010) Regeneration and repair of peripheral nerves with different biomaterials: Review. *Microsurgery* 30:574–588.
61. Palmieri RM, Ingersoll CD, Hoffman MA (2004) The Hoffmann reflex: Methodologic considerations and applications for use in sports medicine and athletic training research. *J Athl Train* 39:268–277.
62. Scheib J, Höke A (2013) Advances in peripheral nerve regeneration. *Nat Rev Neurol* 9:668–676.
63. Ma CHE, et al. (2011) Accelerating axonal growth promotes motor recovery after peripheral nerve injury in mice. *J Clin Invest* 121:4332–4347.
64. Boeltz T, et al. (2013) Effects of treadmill training on functional recovery following peripheral nerve injury in rats. *J Neurophysiol* 109:2645–2657.
65. Ydens E, et al. (2012) Acute injury in the peripheral nervous system triggers an alternative macrophage response. *J Neuroinflammation* 9:176.
66. Mokarram N, Dymanus K, Srinivasan A, English A, Bellamkonda R (2016) Preferential recruitment of anti-inflammatory monocytes significantly enhances peripheral nerve regeneration. *Front Bioeng Biotechnol* 4, 10.3389/conf.FBIOE.2016.01.00186.